© 2014. Published by The Company of Biologists Ltd | Journal of Cell Science (2014) 127, 1726–1737 doi:10.1242/jcs.137695

RESEARCH ARTICLE

Scube2 enhances proteolytic Shh processing from the surface of Shh-producing cells

Petra Jakobs*, Sebastian Exner*, Sabine Schürmann*, Ute Pickhinke, Shyam Bandari, Corinna Ortmann, Sabine Kupich, Philipp Schulz, Uwe Hansen, Daniela G. Seidler and Kay Grobe‡

ABSTRACT

All morphogens of the Hedgehog (Hh) family are synthesized as dual-lipidated proteins, which results in their firm attachment to the surface of the cell in which they were produced. Thus, Hh release into the extracellular space requires accessory protein activities. We suggested previously that the proteolytic removal of N- and C-terminal lipidated peptides (shedding) could be one such activity. More recently, the secreted glycoprotein Scube2 (signal peptide, cubulin domain, epidermal-growth-factor-like protein 2) was also implicated in the release of Shh from the cell membrane. This activity strictly depended on the CUB domains of Scube2, which derive their name from the complement serine proteases and from bone morphogenetic protein-1/tolloid metalloproteinases (C1r/C1s, Uegf and Bmp1). CUB domains function as regulators of proteolytic activity in these proteins. This suggested that sheddases and Scube2 might cooperate in Shh release. Here, we confirm that sheddases and Scube2 act cooperatively to increase the pool of soluble bioactive Shh, and that Scube2-dependent morphogen release is unequivocally linked to the proteolytic processing of lipidated Shh termini, resulting in truncated soluble Shh. Thus, Scube2 proteins act as protease enhancers in this setting, revealing newly identified Scube2 functions in Hh signaling regulation.

KEY WORDS: Sonic hedgehog, Hedgehog acyltransferase, Shedding, Scube

INTRODUCTION

All proteins of the Hedgehog (Hh) family act as powerful morphogens and growth factors during metazoan development. In vertebrates, the Hh family member Sonic Hedgehog (Shh) is essential for the patterning of the ventral neural tube (Briscoe et al., 2001), for specifying digit identities (Ahn and Joyner, 2004; Harfe et al., 2004) and for axon guidance (Charron et al., 2003). In the adult, Hh pathway activation has been implicated in maintaining the stem cell and cancer stem cell niche (Zhao et al., 2009), and in the progression of various cancers (Theunissen and de Sauvage, 2009; Yauch et al., 2008; Zhao et al., 2009). Despite these important roles, various aspects of Hh function remain unclear.

The mode of Hh dispersal in tissues is especially intriguing; all Hh family members are released from the cells in which they are produced, despite having covalent N- and C-terminal lipid modifications (Peters et al., 2004) that result in strong association of Hh proteins with the cell membrane, and the cholesterol-dependent formation of multimeric clusters (Ohlig et al., 2011; Vyas et al., 2008). For initial cholesterol attachment, Shh precursor proteins (called ShhNC, for Shh unprocessed N-terminal signaling and C-terminal autoprocessing domains) undergo internal cleavage that is catalyzed by the Shh C-terminal autoprocessing domain (ShhC, Fig. 1) (Bumcrot et al., 1995; Lee et al., 1994; Liu, 2000; Tabata and Kornberg, 1994). Because ShhNC uses intein-related coupled cleavage and cholesterol esterification (in which extein 1 is ShhN, extein 2 is cholesterol and the intein is ShhC), all resulting 19-kDa proteins generated from the 45-kDa Shh precursor are C-terminal cholesterylated (Liu, 2000; Martí et al., 1995; Porter et al., 1996a; Porter et al., 1996b). The second lipid modification of Hh proteins is the attachment of palmitic acid to the conserved N-terminal cysteine (C85 in fly Hh, C25 in murine Shh) through the primary amine that is exposed after cleavage of the signal peptide (Pepinsky et al., 1998). Such Hh palmitoylation occurs through a thioester intermediate, followed by a spontaneous rearrangement to form the amide. Therefore, Shh proteins lacking N-terminal cysteine (C25S or C25A) are cholesterol-modified but remain unpalmitoylated (Hardy and Resh, 2012). Hh N-acylation requires the expression of a separate gene product, called Hh acyltransferase (Hhat) (Amanai and Jiang, 2001; Chamoun et al., 2001; Lee and Treisman, 2001; Micchelli et al., 2002), a membrane-bound O-acyltransferase (MBOAT) family member. The dual-lipidated fully active Shh product is called ShhNp (Shh N-terminal processed signaling domain). Lipidated Hhs multimerize on the surface of the cells in which they are expressed (Vyas et al., 2008) and are released despite their hydrophobic modifications, whereas other lipidated proteins normally remain tethered to the membrane. Notably, efficient N-palmitoylation is crucial for the binding of the morphogen to its receptor, Patched (Ptc), because unpalmitoylated proteins (Shh expressed in Hhat mutants, or in cysteine to serine or alanine mutants, $ShhNp^{C25S/A}$) are 10–30× less active than wild-type proteins *in vitro* and *in vivo* (Chamoun et al., 2001; Lee et al., 2001). The questions of how Hh lipidation and activity are linked, and how Hh is released despite its dual lipidation are controversial points. Suggested mechanisms include movement by lipoprotein particles (Panáková et al., 2005) and transport by cellular extensions called cytonemes (Bischoff et al., 2013; Roy et al., 2011).

Recently, Scube2-mediated ShhNp extraction and ShhNp ectodomain shedding from the cell surface have also been proposed (Creanga et al., 2012; Dierker et al., 2009; Ohlig et al., 2011; Ohlig et al., 2012; Tukachinsky et al., 2012). The latter mechanism involves

The Institute for Physiological Chemistry and Pathobiochemistry, Westfälische Wilhelms Universität Münster, Waldeyerstrasse 15, D-48149 Münster, Germany.

*These authors contributed equally to this work

‡Author for correspondence (kgrobe@uni-muenster.de)

Received 30 June 2013; Accepted 22 January 2014

Journal of Cell Science

Journal of Cell Science (2014) 127, 1726–1737 doi:10.1242/jcs.137695

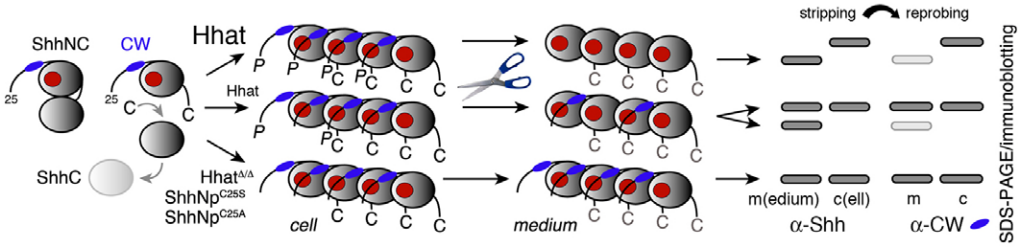

Fig. 1. Model of Shh N-palmitoylation and release. Biosynthesis of ShhNp. The processing of the 45-kDa ShhNC precursor is coupled to cholesterol (C) esterification of all 19-kDa Shh signaling domains generated in the process, resulting in their firm tethering to the cell membrane. Subsequent morphogen multimerization blocks Shh-receptor-binding sites (red circles) by N-terminal peptides. N-palmitoylation (P) of these peptides is catalyzed by Hhat. Impaired palmitoylation [due to insufficient Hhat expression, lack of acyltransferase activity (Hhat$^{\Delta/\Delta}$) or lack of the acceptor cysteine (ShhNp^{C25S}/ShhNp^{C25A})] leaves N-terminal peptides unmodified. This impairs membrane-proximal positioning and the processing of Cardin-Weintraub (CW) motifs (blue), resulting in soluble clusters with their receptor-binding sites still blocked (bottom). The molecular mass of unprocessed proteins thus remains comparable to that of cell-bound precursors, and both forms are detected by α-CW antibodies (bottom, right). By contrast, proteolytic CW processing couples Shh solubilization with the removal of inhibitory N-terminal peptides (top). The associated reduction in the molecular mass of immunoblotted soluble proteins is confirmed by reduced α-CW antibody reactivity (top, right). Partial N-palmitoylation of clusters leads to a higher-molecular-mass band representing α-CW-antibody-reactive unprocessed proteins and a lower-molecular-mass band representing α-CW-antibody-unreactive processed products. Polyclonal α-Shh antibodies detect processed and unprocessed proteins.

A disintegrin and metalloprotease (ADAM)-mediated conversion of cell-surface-tethered ShhNp multimers into truncated morphogen clusters upon membrane-proximal proteolytic removal of lipidated peptide termini (Dierker et al., 2009; Ohlig et al., 2011). Shedding, however, not only removes lipidated peptide anchors for morphogen solubilization but also activates ShhNp (Fig. 1). Initially, in the cell-surface-bound cluster, N-terminal peptides interact with (and block) adjacent binding sites for the Shh receptor, Ptc (Bishop et al., 2009; Bosanac et al., 2009; Farshi et al., 2011; Ohlig et al., 2011), inactivating the unprocessed molecule. By removing N-terminal acylated peptides, sheddases expose the Ptc-binding sites of solubilized clusters and thereby couple Shh release to its activation (Fig. 1). The essential role of N-palmitate for Hh biofunction is therefore indirect; N-acylation is a prerequisite for the membrane-proximal positioning and subsequent shedding of inhibitory N-terminal peptides. Furthermore, by their continued association with the cell membrane, N-palmitoylated inhibitory peptides are completely removed from soluble clusters. Thus, any inhibition of N-palmitoylation prevents N-terminal Hh processing and results in the release of inactive proteins from producing cells (Ohlig et al., 2011; Ohlig et al., 2012).

Scube2 glycoproteins (Signal sequence, cubulin domain, epidermal growth factor 2) also release Shh from transfected 293T cells (Tukachinsky et al., 2012) and HEK293S cells (Creanga et al., 2012). Scube2 is a member of the you-class mutants in zebrafish (Shh is encoded by the sonic-you gene in this species) (Schauerte et al., 1998). *In vitro*, *Xenopus laevis* (x)Scube2 increases Shh solubilization by direct extraction of hydrophobic lipid adducts from the membrane and continued sequestration of these lipids from the aqueous phase (Tukachinsky et al., 2012). By contrast, Scube2Δ, a C-terminal truncation mutant lacking a cysteine-rich and CUB (C1r/C1s, Uegf and Bmp1) domain, does not release Shh (Creanga et al., 2012; Tukachinsky et al., 2012). As one established role of CUB domains is to regulate the assembly of protease–protease-substrate complexes, we hypothesized that Scube2 activity and Shh shedding might be linked. To distinguish between Scube2-linked and Scube2-independent Shh shedding, we analyzed the release of cholesterol-anchored (unpalmitoylated) ShhNp^{C25S} and ShhNp^{C25A} (Hardy and Resh, 2012), and the release of dual-membrane-anchored ShhNp from Hhat-expressing cells. Consistent with reported results (Creanga et al., 2012; Tukachinsky et al., 2012), we found that xScube2 and human (h)Scube2 both increased ShhNp^{C25S} and ShhNp^{C25A} solubilization. However, xScube2 did not release dual-lipidated ShhNp, and hScube2 showed only limited activity. Notably, hScube2- or xScube2-solubilized morphogens always lacked their lipidated peptide termini, suggesting that Scube2 activity is strictly linked to proteolytic Shh processing at the cell surface. Indeed, Scube2-mediated Shh solubilization was further enhanced by activated shedding, suggesting that although Scube2 activity clearly contributes to Shh solubilization, this can be bypassed by increased proteolytic activity that results in the same processed morphogens. This finding is consistent with other CUB-domain proteins acting as protease enhancers, and resolves the apparent contradiction between sheddase- and Scube2-mediated Shh release *in vitro*.

RESULTS

ShhNp clusters dissociate into proteins with different electrophoretic mobilities

Both in vertebrates and in *Drosophila melanogaster*, N-palmitoylation of Hh proteins is absolutely required for unimpaired binding to the Ptc receptor and for biofunction. Therefore, thorough biochemical characterization of recombinant Shh must avoid any effects caused by an insufficient level of post-translational palmitoylation. It is known that strong Shh expression in mammalian or insect cells exceeds the palmitoylation capacities of endogenous Hhat (Pepinsky et al., 1998). By contrast, Shh expression in cultured mammalian cells using a moderately active (non-viral) promoter increases dual lipidation (Taipale et al., 2000). By semi-quantitative reverse transcriptase (RT)-PCR, we confirmed low or virtually absent *hhat* expression in HEK293 and Bosc23 cells (Fig. 2). Even after repeated rounds of nested PCR, *hhat* expression was only detected in CHO-K1 cells and, at very low levels, in Bosc23 cells. By contrast, dispatched (*Disp*) mRNA was expressed in all cell lines. This suggests that transfection of HEK293 and Bosc23 cells with Shh constructs under the control of a strong (viral) promoter results in substantial amounts of unpalmitoylated (but fully cholesterylated) ShhNp. This scenario

Journal of Cell Science (2014) 127, 1726–1737 doi:10.1242/jcs.137695

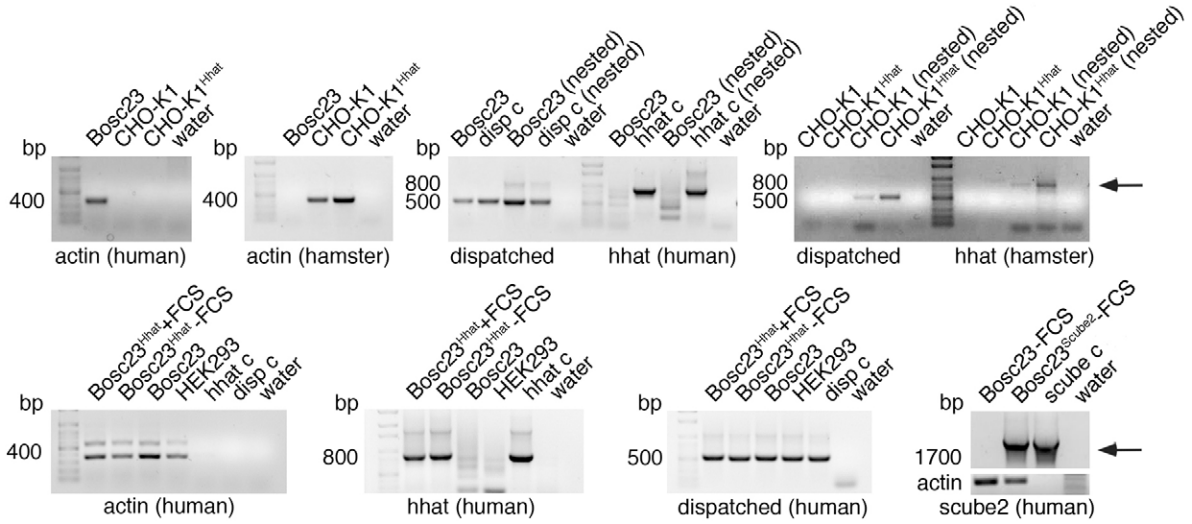

Fig. 2. Dispatched, scube2 and *hhat* mRNA expression in Bosc23, HEK293 and CHO-K1 cells. Results of semi-quantitative RT-PCR analyses are shown. For low-abundance transcripts, results of a second (nested) PCR are also shown. Note that *hhat* expression is low or absent in all cell lines. By contrast, control Hhat-transfected cells (CHO-K1^{Hhat} or Bosc23^{Hhat}) express *hhat* under normal culture conditions and under serum-free conditions (-FCS). Note that dispatched mRNA was detected in all cell lines, but *scube2* was not detected in Scube2-untransfected Bosc23 cells. Actin served as a loading control. Hhat c, scube c and disp c are positive controls (*hhat*, *scube2* and *disp* cDNAs).

was confirmed in both cell lines (supplementary material Fig. S1A).

Hhat coexpression enhances ShhNp processing and biofunction

To increase the N-acylation of recombinant protein, we employed bicistronic mRNA constructs for the coupled expression of ShhNp and Hhat in Bosc23 cells (Fig. 3A). ShhNp was also expressed from pIRES in the absence of exogenous Hhat (Fig. 3A). We then determined the relative ShhNp acylation levels by reverse-phase high-performance liquid chromatography (HPLC) on a C4 column (Pepinsky et al., 1998). As shown in Fig. 3B, negative control ShhN^{C25S} lacking both N-linked palmitate and C-linked cholesterol eluted

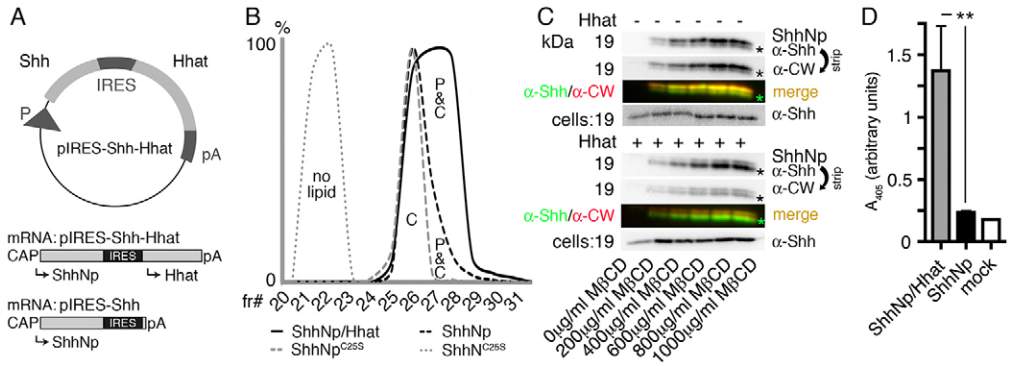

Fig. 3. ShhNp/Hhat coexpression increases N-terminal palmitoylation and processing. (A) pIRES constructs for transfection of Bosc23 cells. ShhNp translation from bicistronic mRNA was cap-dependent, Hhat translation was cap-independent. P, promotor; IRES, internal ribosomal entry site; pA, polyadenylation site. As a control, Shh was expressed from the same vector without Hhat (pIRES-Shh). (B) Analysis of ShhNp lipid modifications by reverse-phase HPLC. Lysates of cells expressing non-lipidated ShhN^{C25A}, cholesterol-modified ShhNp^{C25A} (indicated by 'C') and ShhNp in the presence or absence of exogenous Hhat were eluted from a C4 column by using an increasing acetonitrile gradient. Fractionated proteins were precipitated and analyzed by SDS-PAGE and immunoblotting. Elution profiles are expressed relative to the highest protein amount in a given fraction (set to 100%). pIRES-Shh-Hhat-expressed proteins show enhanced N-palmitoylation (indicated by 'P&C'). The majority of ShhNp expressed in the absence of exogenous Hhat is only cholesterol modified. (C) Dose-dependent MβCD-induced ShhNp shedding from Bosc23 cells. Conditioned media and the corresponding cell lysates were analyzed by immunoblotting using anti-Cardin-Weintraub antibodies (α-CW) and anti-Shh (α-Shh) antibodies. pIRES-Shh-Hhat-expressed products were N-terminally processed during release, as shown by their reduced molecular mass and impaired α-CW antibody reactivity (asterisks). To better demonstrate processing during release, grayscale blots were inverted and colored (green, α-Shh signal; red, α-CW signal). Yellow or orange signals in merged blots thus denote the unprocessed protein fraction. Green signals confirm the removal of (most) N-terminal CW residues from processed proteins. N-terminal Shh processing in the absence of exogenous Hhat was limited, as indicated by a predominant yellow (upper) band. (D) Processed ShhNp (from pIRES-Shh-Hhat-transfected cells, green) is significantly more active than comparable amounts of ShhNp expressed in cells lacking exogenous Hhat expression (pIRES-Shh). Levels of Shh-induced alkaline phosphatase activity in C3H10T1/2 cells are measured as absorption at 405 nm, serving as a readout for C3H10T1/2 differentiation. Data are expressed in arbitrary units and shown as means±s.e.m. $^{**}P<0.01$. One representative result out of three independent experiments is shown.

Journal of Cell Science (2014) 127, 1726–1737 doi:10.1242/jcs.137695

first (in fraction 22), and cholesterylated ShhNp^{C25S} eluted in fraction 26. Notably, about 75% of pIRES-Shh-expressed protein also eluted in fraction 26, suggesting single cholesterol modification ('C' in Fig. 3B), and only about 25% of pIRES-Shh-expressed protein was detected in fractions 27 and 28, where the dual-modified form would be expected to elute ('P&C' in Fig. 3B). By contrast, >70% of Hhat-coexpressed ShhNp (referred to herein as ShhNp/Hhat) eluted in fraction 28, characteristic of the dual-lipidated protein. Thus, pIRES-mediated coexpression of the acyltransferase and the ligand increases the throughput of post-translational palmitoylation. Because of the essential functional roles of N-palmitate in Hh biology (Chamoun et al., 2001; Chen et al., 2004), we employed Hhat and ShhNp coexpression for all further ShhNp release and bioactivity assays *in vitro*.

First, we confirmed that the proteolytic processing of cell-tethered ShhNp was increased as a consequence of increased N-palmitoylation. Where indicated, methyl-β-cyclodextrin (MβCD) was added to activate endogenous cell-surface sheddases (Dierker et al., 2009; Kojro et al., 2001; Matthews et al., 2003; Nishie et al., 2012; Parkin et al., 2004; von Tresckow et al., 2004; Walev et al., 2000; Zimina et al., 2005). This treatment resulted in two soluble ShhNp proteins, of differing electrophoretic mobilities, derived from one cellular precursor. Hhat coexpression increased the proportion of the higher electrophoretic mobility protein in solution (Fig. 3C, lower panels). To prove that N-terminal processing of these proteins was occurring, blots were stripped and re-incubated with anti (α)-CW antibodies raised against the N-terminal Cardin-Weintraub peptide $K^{33}RRHPKK^{39}$ (see Fig. 1) (Ohlig et al., 2012). α-CW antibodies still bind to the C-terminal CW-peptide fragment $R^{35}HPKK^{39}$, but do not detect $H^{36}PKK^{39}$ CW peptides that lack amino acid R^{35} (supplementary material Fig. S1B). Therefore, α-CW antibodies detect soluble proteins lacking up to ten N-terminal amino acids, whereas the proteolytic removal of additional amino acids abolishes the binding of these antibodies. Indeed, as shown in Fig. 3C, α-CW antibodies detected unprocessed soluble Shh, but did not detect truncated proteins released from Hhat-co-transfected Bosc23 cells. For better visualization of N-terminal Shh processing in this and subsequent experiments, α-Shh- and α-CW-incubated blots were electronically inverted, false-colored and merged. Comparable binding of α-Shh antibodies (green) and α-CW antibodies (red) thus marks unprocessed proteins in yellow, and polyclonal α-Shh antibody binding, combined with strongly impaired α-CW antibody binding, confirms N-terminal protein processing (Fig. 3C).

Our model of coupled ShhNp truncation and activation predicted that the processed ShhNp released from Hhat-coexpressing cells would have the strongest bioactivity. To test this possibility, we used the Shh-responsive murine cell line C3H10T1/2 (Nakamura et al., 1997) (supplementary material Fig. S2). As shown in Fig. 3D, truncated ShhNp strongly induced the production of alkaline phosphatase as a readout for C3H10T1/2 differentiation (1.371±0.36 arbitrary units for ShhNp/Hhat compared to 0.235±0.015 arbitrary units for ShhNp clusters of both processed and unprocessed protein, $P<0.01$, $n=6$, ±s.e.m). By contrast, media from mock-transfected cells (0.18±0.005 arbitrary units) were inactive. Thus, we confirmed that N-palmitate plays an essential yet indirect role in the conversion of cell-bound ShhNp clusters into Ptc-binding soluble forms, and that Hhat activation increases this conversion (Fig. 1).

Sheddases release dual-lipidated ShhNp from producing cells

The data from two recent studies suggest that Shh is secreted by the sequential action of Dispatched and Scube2, possibly through disruption of cholesterol-membrane interactions (Creanga et al., 2012; Tukachinsky et al., 2012). This is supported by efficient xScube2-mediated release of cholesterol-modified (but unpalmitoylated) HaloTag proteins from the cell surface (Tukachinsky et al., 2012). These reports prompted us to directly compare sheddase- and xScube2-mediated ShhNp release from transfected cells (Fig. 4A). To this end, Bosc23 cells were Shh-transfected in the presence or absence of Hhat and together with xScube2 or xScube2Δ, the latter lacking the C-terminal CUB-domain (Tukachinsky et al., 2012). After 30 h, cells were washed and serum-free medium was added, and the cells were incubated for a further 14 h to allow protein expression. Where indicated, 400 µg/ml MβCD was also added to induce shedding. After 14 h, the media were ultracentrifuged and subjected to SDS-PAGE and immunoblotting. Cell lysates were analyzed for Shh expression, and α-hemagglutinin (α-HA) antibodies were used to confirm the expression of HA-tagged xScube2 and xScube2Δ proteins. Under these conditions, we did not observe significant xScube2-mediated ShhNp release in the absence of MβCD (Fig. 4A, lanes 5, 6, 11, 12). By contrast, MβCD strongly increased morphogen solubilization independently of Scube2 function. Consistent with the data shown in Fig. 3C, solubilized ShhNp that was coexpressed with Hhat showed reduced α-CW antibody reactivity (Fig. 4A). Moreover, little ShhNp was released from Hhat-coexpressing Bosc23 cells, suggesting that the N-terminal processing of N-palmitoylated proteins might constitute a rate-limiting step in Shh release (Fig. 4A, compare lanes 1–4 to lanes 7–10). ImageJ quantification of immunoblotted soluble and cell-bound proteins revealed strongly impaired ShhNp/Hhat solubilization, independent of Scube2 function (the amount of soluble proteins as a percentage of the amount of cell-tethered proteins: ShhNp/Hhat 103%±6%, ShhNp 500%±30%, $P=0.0002$, $n=3$). Another independent experiment showed similar results (ShhNp/Hhat 112%±12%, ShhNp 670%±63%, $P<0.0001$, $n=8$).

Next, we assayed the bioactivities of solubilized proteins at the concentrations shown in Fig. 4A. Processed (lanes 1–4) and mixed processed and unprocessed (lanes 7–10) clusters induced C3H10T1/2 differentiation to comparable levels, despite the excess of mixed processed and unprocessed ShhNp (Fig. 4B, upper panel). This is explained by the enhanced bioactivity of processed ShhNp and the inactivity of the unprocessed protein fraction. Protein normalization prior to C3H10T1/2 incubation (to rule out concentration-dependent morphogen effects) supports this result (Fig. 4B, lower panel). Thus, we confirmed that N-terminally processed clusters are significantly more active than comparable amounts of largely unprocessed proteins. Note that the N-terminal CW sheddase target site also represents the binding site for heparan sulfate proteoglycans on the surface of Shh-producing cells (Chang et al., 2011; Farshi et al., 2011; Vyas et al., 2008); this suggests a possible mode of regulation of Shh release.

Cholesterylated unpalmitoylated ShhNp^{C25A} is solubilized by xScube2

We next investigated the xScube2-mediated solubilization of cholesterol-modified proteins (Tukachinsky et al., 2012). To this end, we compared the relative solubilization of ShhNp/Hhat

Journal of Cell Science (2014) 127, 1726–1737 doi:10.1242/jcs.137695

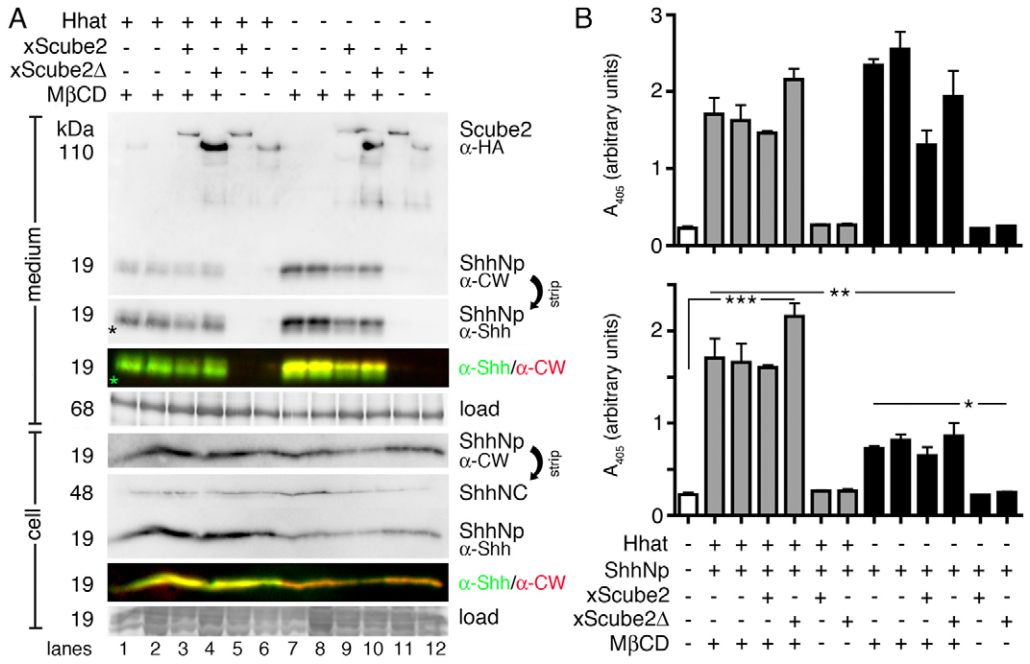

Fig. 4. xScube2- and sheddase-mediated ShhNp release from Hhat-overexpressing cells. (A) Bosc23 cells were transfected with pIRES-Shh-Hhat or pIRES-Shh together with xScube2 or inactive xScube2Δ. After 30 h, cells were washed, and serum-free DMEM was added for 14 h in the presence or absence of 400 μg/ml MβCD. MβCD strongly induced N-terminal truncation of Hhat-coexpressed ShhNp (lanes 1–4), as shown by reduced α-CW antibody reactivity of soluble proteins (asterisk, green bands in the merged color picture). MβCD strongly released N-terminally unprocessed ShhNp as well (lanes 7–10, yellow bands). xScube2 did not enhance ShhNp release [lanes 3, 5, 9 and 11 (xScube2) versus lanes 4, 6, 10 and 12 (xScube2Δ)]. Note that lipidated ShhNp was strongly enriched on the surface of Hhat-coexpressing cells, indicating that membrane-associated N-palmitate restricts the release of unprocessed and incompletely processed clusters. (B) All conditioned media (as shown in A) induced C3H10T1/2 cell differentiation to comparable levels, despite higher amounts of (largely) unprocessed soluble proteins in media from Hhat-negative cells (for fully processed ShhNp/Hhat the data are 1.7±0.2, 1.6±0.02, 1.45±0.022 and 2.16±0.14 arbitrary units, mock 0.22±0.02 arbitrary units, $P \leq 0.0004$; and for mixed ShhNp the data are 2.3±0.08, 2.56±0.22, 1.3±0.2 and 1.9±0.33 arbitrary units, $P \leq 0.0012$). After protein normalization, N-processed forms showed significantly elevated bioactivities [for largely processed ShhNp/Hhat the data are 1.8±−0.2, 1.7±−0.2, 1.6±−0.02 and 2.2±−0.14 arbitrary units, $P \leq 0.0004$; for ShhNp alone (only partially processed) the data are 0.72±0.03, 0.81±0.06, 0.65±0.1 and 0.86±0.14 arbitrary units, $P \leq 0.0027$]. The data show the means±s.d. *$P<0.05$, **$P<0.01$ and ***$P<0.0003$. One representative result out of three independent experiments is shown.

(dual-membrane-anchored), ShhNp (mixed cluster consisting of processed and unprocessed morphogen) and unpalmitoylated ShhNp^{C25A} [only cholesterol-anchored (Hardy and Resh, 2012)] in the presence or absence of 400 μg/ml MβCD and xScube2 or xScube2Δ. xScube2, but not xScube2Δ, slightly enhanced the release of cholesterylated, N-terminally unprocessed ShhNp^{C25A} both in the presence (Fig. 5A, lane 11) and absence (Fig. 5A, lane 5) of MβCD. The release of N-palmitoylated proteins, however, was not increased by xScube2 (Fig. 5A, lanes 1, 3, 7, 9). By contrast, the sheddase activator MβCD enhanced the release and N-truncation of ShhNp/Hhat, as indicated by a molecular mass shift and the loss of α-CW antibody reactivity (Fig. 5A, lanes 7–8). Consistent with the removal of inhibitory N-terminal peptides from the solubilized cluster, truncated ShhNp/Hhat showed the strongest Shh pathway activation in C3H10T1/2 cells, and ShhNp expressed in the absence of Hhat showed limited processing and activity (Fig. 5B). The bioactivities of unprocessed ShhNp^{C25A} were even further reduced (1.3±0.02 and 1.7±0.1 arbitrary units for ShhNp/Hhat, $P=0.0003$ and 0.0005, $n=3$; 0.9±0.005 and 0.86±0.14 arbitrary units for ShhNp, $P=0.001$ and 0.027, $n=3$; and 0.28±0.03 and 0.43±0.09 arbitrary units for ShhNp^{C25A}, $P=0.047$ and 0.03, $n=3$, after protein normalization, ±s.e.m., Fig. 5B, lower panel). As observed earlier (Fig. 4A), the amount of soluble ShhNp^{C25A} was ~3–12-fold higher than the amount of soluble ShhNp [soluble protein amount as a percentage of the amount of cell-tethered proteins: ShhNp/Hhat 50%±7%, ShhNp 191%±2%, ShhNp^{C25A} 580%±46% (Fig. 5A)]. The same result was obtained from ShhNp- and ShhNpC25A-expressing CHO-K1 and CHO-K1 Hhat cells. These results support the selective release of ShhNp C-termini by xScube2, and they show that this process is further enhanced by MβCD. This suggests that xScube2 and sheddase activities at Shh C-termini are independent but additive, or that xScube2 and sheddases cooperate to mediate ShhNp^{C25A} release.

xScube2 enhances C-terminal shedding of ShhNp^{C25A}

To distinguish between these two possibilities, we monitored the release of ShhNp^{C25A} carrying N- and C-terminal HA tags (Fig. 6A). The addition of the tags resulted in the production of an extended ShhNp$^{C25A;HA}$ C-terminal membrane anchor, N^{190}SVAAKSG-*YPYDVPDYA*-G^{198} (in which G^{198} represents the cholesterol-modified glycine and the italicized letters represent the tag), and the ShhNp$^{C25A;\Delta HA}$ fragment N^{190}-*YPYDVPDYA*-G^{198} upon deletion of the C-terminal Shh fragment. As a control, we expressed ^{HA}ShhNp^{C25S} (Ohlig et al., 2011). This construct carried an internal HA tag between residues G^{32} and the first CW residue, K33, resulting in the N-terminal sequence S^{25}GPGRGFG-*YPYDVPDYA*-KRRHPKK^{39}. All morphogen variants lacked the palmitate acceptor C25, resulting in the secretion of monolipidated (cholesterylated)

Journal of Cell Science (2014) 127, 1726–1737 doi:10.1242/jcs.137695

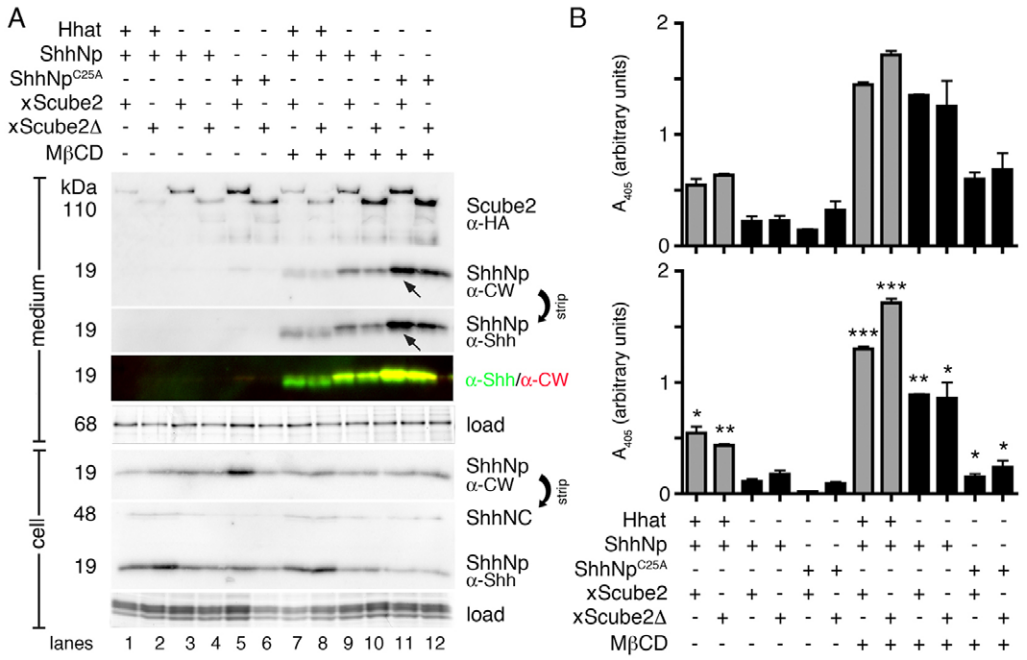

Fig. 5. xScube2 releases cholesterylated yet unpalmitoylated ShhNp^{C25A}. (A) Western blots of conditioned media from Bosc23 cells transfected with pIRES-Shh-Hhat, pIRES-Shh or ShhNp^{C25A}, together with xScube2 or xScube2Δ, using α-CW and α-Shh. Where indicated, MβCD was added to induce shedding. The strongest MβCD-induced protein release was observed for ShhNp^{C25A} (lanes 11 and 12, yellow signals in the merged color picture) in combination with xScube2 (arrow). Amounts of soluble ShhNp^{C25A} and ShhNp were increased over those of N-processed ShhNp derived from Hhat-expressing cells (lanes 7 and 8, green signals). Load, gel-loading control [BSA (medium) and cellular proteins]. (B) MβCD-released proteins were bioactive (upper panel). The levels of alkaline phosphatase expression induced by the conditioned media shown in A indicate that C3H10T1/2 cells are undergoing differentiation and hence give a readout of morphogen bioactivity. Notably, low amounts of Hhat-coexpressed ShhNp showed strong bioactivities even in the absence of MβCD (A, lanes 1 and 2). xScube2-released ShhNp^{C25A} was much less active (A, lanes 5 and 6). After protein normalization, MβCD-released processed ShhNp/Hhat showed significantly enhanced bioactivity compared with all other (largely unprocessed) proteins (lower panel). Lane 1, P=0.01; lane 2, P=0.001; lane 7, 0.0003; lane 8, P=0.0005; lane 9, P=0.0011; lane 10, P=0.0027; lane 11, P=0.03; lane 12, P=0.047 when compared with unprocessed ShhNpC25S (lane 5). Data are expressed as means±s.e.m. *P<0.05, **P<0.01 and ***P<0.001.

proteins. The proteins were expressed for 6 h in serum-free DMEM as described previously (Tukachinsky et al., 2012), and were analyzed by immunoblotting together with the Bosc23 cell lysate. The deletion of the C-terminal Shh fragment strongly impaired the release of ShhNp$^{C25A;\Delta HA}$ (the ratio of soluble to cell-bound protein was 1.156±0.3 arbitrary units for ShhNp$^{C25A;\Delta HA}$ compared to 6.2±0.8 arbitrary units for ^{HA}ShhNp^{C25S}; P=0.0001; n=8) (Fig. 6B,C). However, the

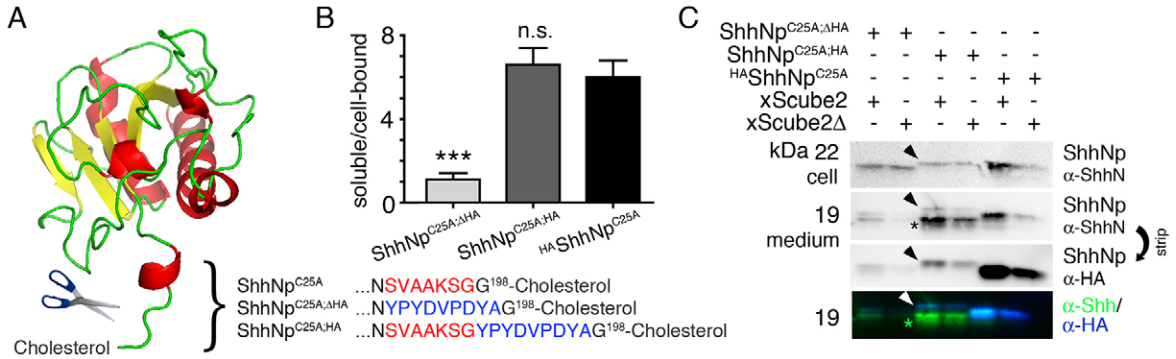

Fig. 6. xScube2 enhances C-terminal ShhNp processing. (A) A model of the protein structure of Shh, showing that the extended membrane-anchored Shh C-terminal peptide represents an accessible sheddase target site (Protein Data Bank ID1VHH). Expressed proteins include N-terminally HA-tagged ^{HA}ShhNp^{C25A}, ShhNp$^{C25A;HA}$ carrying a C-terminal HA insertion (blue) and ShhNp$^{C25A;\Delta HA}$, where the C-terminal peptide (red) is replaced by the tag. (B) Proteins were expressed in Bosc23 cells and the release of soluble versus cell-bound forms was compared. The replacement of the Shh C-terminal amino acids with HA, but not HA insertion, strongly impaired Shh release. Data show the means±s.d. ***P<0.001; n.s., non-significant. (C) Immunoblot analyses of cell-tethered proteins (cell) and those released into serum-free DMEM after 6 h (medium) using α-ShhN and α-HA antibodies. No MβCD was added. Soluble 21.4-kDa ^{HA}ShhNp^{C25A} was recognized by both antibodies; 19.6-kDa truncated ShhNp$^{C25A;\Delta HA}$ and ShhNp$^{C25A;HA}$ were detected by α-ShhN antibodies but not by α-HA antibodies. Bands are artificially colored to reveal the proteins recognized by the different antibodies. Note that the additional Scube2-released protein fraction was also C-terminally processed (asterisks). Arrowheads denote unprocessed proteins not fully removed by ultracentrifugation. Data shown are one representative result out of eight independent experiments.

Journal of Cell Science

Journal of Cell Science (2014) 127, 1726–1737 doi:10.1242/jcs.137695

insertion of the HA tag downstream of this peptide did not impair $ShhNp^{C25A;HA}$ release (6.8±0.83 arbitrary units, $P=0.6$, $n=8$). The reduced $ShhNp^{C25A;\Delta HA}$ solubilization is best explained by impaired proteolytic processing of the proline-rich HA-tag that replaced the original sheddase target site, consistent with strongly divergent physicochemical properties of the two peptide sequences (GRAVI hydropathicity index of the HA-tag is −0.9, versus 0.19 for the hydrophobic Shh C-terminus; the pI of the HA-tag is 3.56, versus 8.47 for the Shh C-terminus). These differences might impair the proteolytic processing of recombinant Shh protein variants on the cell surface.

Fig. 6C illustrates the proteolytic cleavage of C-terminal Shh peptides during release. α-HA antibodies (blue) and α-Shh antibodies (green) both detected N-terminally tagged $^{HA}ShhNp^{C25S}$ in western blots of cell lysates and supernatants (right lanes, bright blue signals in merged blots). This is consistent with impaired N-terminal processing of unpalmitoylated $ShhNp^{C25S}$. By contrast, 22-kDa $ShhNp^{C25A;HA}$ was truncated to a 19-kDa soluble form that completely lacked α-HA antibody reactivity (Fig. 6C). Note that xScube2 enhanced the C-terminal processing of $ShhNp^{C25A;HA}$. The alternative possibility of independent sheddase and xScube2 function was never observed; additional $ShhNp^{C25A;HA}$ released by xScube2 always lacked α-HA antibody reactivity. The same result was observed for xScube2-released $ShhNp^{C25A;\Delta HA}$ (Fig. 6C, lane 1).

Human Scube2-enhances N- and C-terminal ShhNp shedding

In contrast to xScube2-enhanced Shh C-terminal release (Tukachinsky et al., 2012), Creanga et al. reported that mScube2 mediates the release of cholesterol- and palmitoyl-modified Shh from HEK293S cells (Creanga et al., 2012). We hypothesized that the observed difference might stem from the use of amphibian versus mammalian Scube2 in a mammalian expression system, and we tested this idea by coexpressing ShhNp with FLAG-tagged human (h)Scube2 (Tsai et al., 2009). As observed previously for xScube2, hScube2 solubilized non-palmitoylated $ShhNp^{C25S}$, and hScube2Δ (lacking the C-terminal cysteine-rich- and CUB-domain) was less active (Fig. 7A). In addition, we observed increased solubilization of dual-lipidated ShhNp/Hhat and of N-palmitoylated non-cholesterylated ShhN/Hhat into hScube2-conditioned serum-free medium after 6 h (Fig 7A,B). Importantly, the majority of Scube2-solubilized proteins lacked α-CW antibody reactivity, consistent with

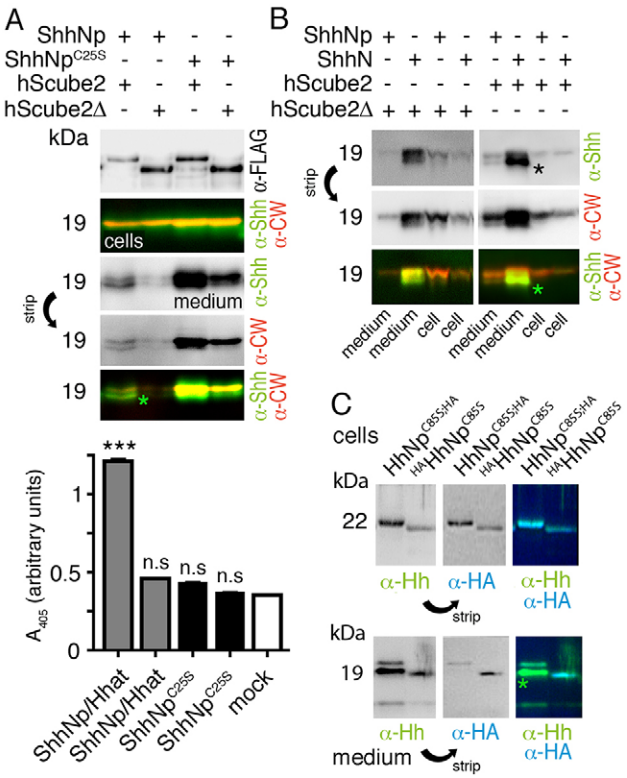

Fig. 7. Release of vertebrate Hhs in the presence of Scube2, and of invertebrate Hhs in the absence of Scube2. (A) ShhNp processing is increased by hScube2. Upper panel, western blots of Bosc23 cells transfected with pIRES-Shh-Hhat or $ShhNp^{C25A}$, and co-transfected with hScube2 or hScube2Δ, using α-Shh (green) and α-CW (red) antibodies . Bands are artificially colored to reveal the proteins recognized by the different antibodies. No MβCD was added. The strongest protein release was observed for N-terminally unprocessed $ShhNp^{C25A}$ in combination with hScube2 (yellow signals). Notably, hScube2 also increased ShhNp solubilization, linked to N-terminal processing (green band, asterisk). Lower panel, hScube2-solubilized truncated proteins were bioactive, as defined by alkaline phosphatase expression by C3H10T1/2 cells in response to treatment with conditioned media from transfected Bosc23 cells. Data show the means±s.d. ***$P<0.001$; n.s., non-significant. (B) ShhN lacking the C-terminal autoprocessing domain was coexpressed with Hhat in Bosc23 cells. This generated palmitoylated and non-cholesterylated morphogens undergoing hScube2-dependent N-terminal processing during release (green band, asterisk). (C) Immunoblot of HA-tagged *Drosophila* HhNp expressed in S2 cells, using α-Hh antibodies (green) and α-HA antibodies (blue). Bands are artificially colored to reveal the proteins recognized by the different antibodies. No MβCD was added. Right: Immunoblot analysis of proteins released into serum-free S2 cell media after 14 h. Solubilized 22-kDa $^{HA}HhNp^{C85S}$ reacted with both antibodies, but truncated 19-kDa $HhNp^{C85S;HA}$ was only detected by α-Hh antibodies. Loss of α-HA antibody reactivity is consistent with C-terminal shedding. The asterisk (*) indicates processed soluble protein lacking the HA-tag. One representative result out of three independent experiments is shown.

strong ShhNp bioactivity in the C3H10T1/2 reporter cells (1.2±0.02 arbitrary units for ShhNp coexpressed with hScube2, versus 0.46±0.05 arbitrary units for ShhNp coexpressed with hScubeΔ; $P<0.0001$; 0.35±0.06 arbitrary units in the mock control; $n=4$; ±s.d.; Fig. 7A). We thus conclude that mammalian hScube2 activates N-terminal and C-terminal shedding, whereas xScube2 activity is restricted to the Shh C-terminus. Sequence comparison of full-length hScube2 and xScube2 revealed 71% sequence identity and 80% identity and similarity on the protein level, and comparison of the CUB domains revealed 96% sequence identity and 99% protein identity and similarity. This is consistent with their conserved role in ShhNp release, and suggests that the observed functional differences between xScube2 and hScube2 are probably not explained by these domains. Notably, the lack of Scube2 expression in Bosc23 cells (Fig. 2) is consistent with ShhNp insolubility under normal culture conditions, and with the increased release of ShhNp that is mediated by the unspecific sheddase activator MβCD; the use of MβCD might override the requirement for Scube2 function (Figs 3–5).

C-terminal HhNp shedding in *Drosophila* S2 cells is independent of Scube2

We wondered whether Hh shedding occurs in organisms that completely lack Scube protein function. To answer this question, we expressed C-terminally HA-tagged *Drosophila* HhNp in *Drosophila* S2 cells, and analyzed the cell-bound and soluble material as described above. Notably, C-terminal cholesterol modification and N-palmitoylation (at amino acid C85 in *Drosophila*) are conserved between vertebrate and invertebrate Hh family members (Chamoun et al., 2001; Guerrero and Chiang, 2007). However, Scube proteins are present only in vertebrates (Tukachinsky et al., 2012). This raises the question of how invertebrates secrete Hh. As shown in Fig. 7C, α-Hh and α-HA antibodies detected ^{HA}HhNp^{C85S} and HhNp$^{C85S;HA}$ in cell lysates. In solution, ^{HA}HhNp^{C85S} (N-terminally HA-tagged and cholesterylated) was also detected by both α-HA antibodies and α-Hh antibodies, consistent with impaired N-terminal shedding of unpalmitoylated proteins. By contrast, HhNp$^{C85S;HA}$ (the C-terminally HA-tagged and cholesterylated protein) was truncated to 19-kDa soluble forms that were not detected by α-HA antibodies, as shown previously for the vertebrate ortholog. Thus, for the first time, we demonstrate the proteolytic shedding of cholesterylated HhNp from invertebrate cells. This finding explains the recent observation of bioactive sterol-free Hh morphogens *in vitro* and in *Drosophila* (Palm et al., 2013). We conclude that, in *Drosophila* S2 cells, C-terminal processing of the Hh morphogen occurs in the absence of Scube2, consistent with the suggested role of Scube2 as a sheddase enhancer. Consistent with deep phylogenetic divergence between vertebrates and insects, and with the lack of any Scube ortholog in the fly, exogenous xScube2 or hScube2 proteins failed to increase HhNp release from transfected S2 cells (supplementary material Fig. S3).

To exclude possible processing artifacts caused by the inserted HA tags, we next analyzed dual-lipidated ShhNp/Hhat, C-lipidated ShhNp^{C25A} and non-lipidated ShhN$^{C25S;*190}$ (the latter mimicking C-terminal truncation at position N190) by reverse-phase HPLC (Pepinsky et al., 1998). As already shown in Fig. 3B, cell-tethered monolipidated and dual-lipidated proteins could be easily distinguished from non-lipidated forms (Fig. 8A). To directly test delipidation during solubilization, proteins were secreted into serum-free medium for 12 h, ultracentrifuged to remove membranous remnants, and were then processed as described above for the cell pellet. As expected, the most soluble ShhNp/Hhat and ShhNp^{C25A} co-eluted with ShhN$^{C25S;*190}$ (Fig. 8A). All three elution peaks showed comparable tailing, possibly owing to unspecific secondary retention effects or residual silanol interactions (supplementary material Fig. S4). Nevertheless, our finding that the majority of solubilized ShhNp/Hhat and ShhNp^{C25A} eluted in fractions that were characteristic of the non-lipidated morphogen confirms the loss of cholesterol by C-terminal proteolytic processing (and loss of palmitate by N-terminal proteolytic processing). The comparable elution profiles of solubilized monolipidated ShhNp$^{C25A;HA}$ and dual-lipidated ShhNp/Hhat expressed in the presence of xScube2 (Fig. 8B) further support our findings. Finally, fully processed ShhNp that was released in the presence of xScube2 (inset in Fig. 8C) showed the strongest bioactivity in C3H10T1/2 cells [1.183 arbitrary units, $P=0.0001$ for ShhNp/Hhat coexpressed with xScube2; 0.4±0.036 arbitrary units, $P=0.0006$ for ShhNp coexpressed with xScube2; 0.2±0.0005 arbitrary units, $P=0.45$ for ShhNp^{C25S} coexpressed with xScube2; 0.21±0.014 arbitrary units for mock; all $n=6$; ±s.d.) even at the unadjusted concentrations shown in the inset (Fig. 8C).

Finally, we employed gel-filtration chromatography to test our hypothesis versus the alternative model in which continued ShhNp–xScube2 association is a prerequisite for Shh solubilization (Tukachinsky et al., 2012). The underlying idea was that if continued Shh–xScube2 interactions in solution shield cholesterol from the aqueous environment, then monomeric (20 kDa) lipidated ShhNp should never be present in solution, and a substantial portion of coexpressed 112-kDa xScube2 should colocalize with ShhNp. However, under the serum-free conditions employed, this was not the case; Shh that was solubilized by xScube2 was largely monomeric in solution (Fig. 8D), consistent with a previous report (Chen et al., 2004). By contrast, the size distributions of xScube2 and xScube2Δ were highly variable (Fig. 8E), consistent with Ca^{2+}-modulated, epidermal growth factor (EGF)-domain-mediated Scube aggregation in solution (Tu et al., 2008). Taken together, these observations suggest an alternative to models of lipid-mediated transport in micelles or continued equimolar xScube2–Shh complexation, because both would predict ShhNp complexes of >100-kDa and the absence of monomeric ShhNp in solution. We explain the loss of the terminal peptides and associated lipids from monomeric soluble Shh by cell-surface shedding, and postulate that Scube2 enhances this process (Fig. 8F).

DISCUSSION

In this work, we show that the post-translational N-acylation of Bosc23-overexpressed Shh is incomplete under normal culture conditions. The coexpression of ShhNp and the N-acyltransferase Hhat in Bosc23 cells restores Shh N-palmitoylation and processing, resulting in enhanced biofunction of the morphogen compared with that of incompletely acylated or unmodified clusters. Moreover, we found that the amount of soluble ShhNp^{C25A} significantly exceeded the amount of soluble dual-lipidated protein. This suggests that N-palmitoylated peptides contribute to the association of Shh with cell membranes and that their processing might control Shh release. This is consistent with enhanced plasma membrane association of Spitz, an N-acylated EGF-like molecule in flies (Miura et al., 2006), and with increased *Drosophila* HhNp release upon RNAi-mediated

Journal of Cell Science (2014) 127, 1726–1737 doi:10.1242/jcs.137695

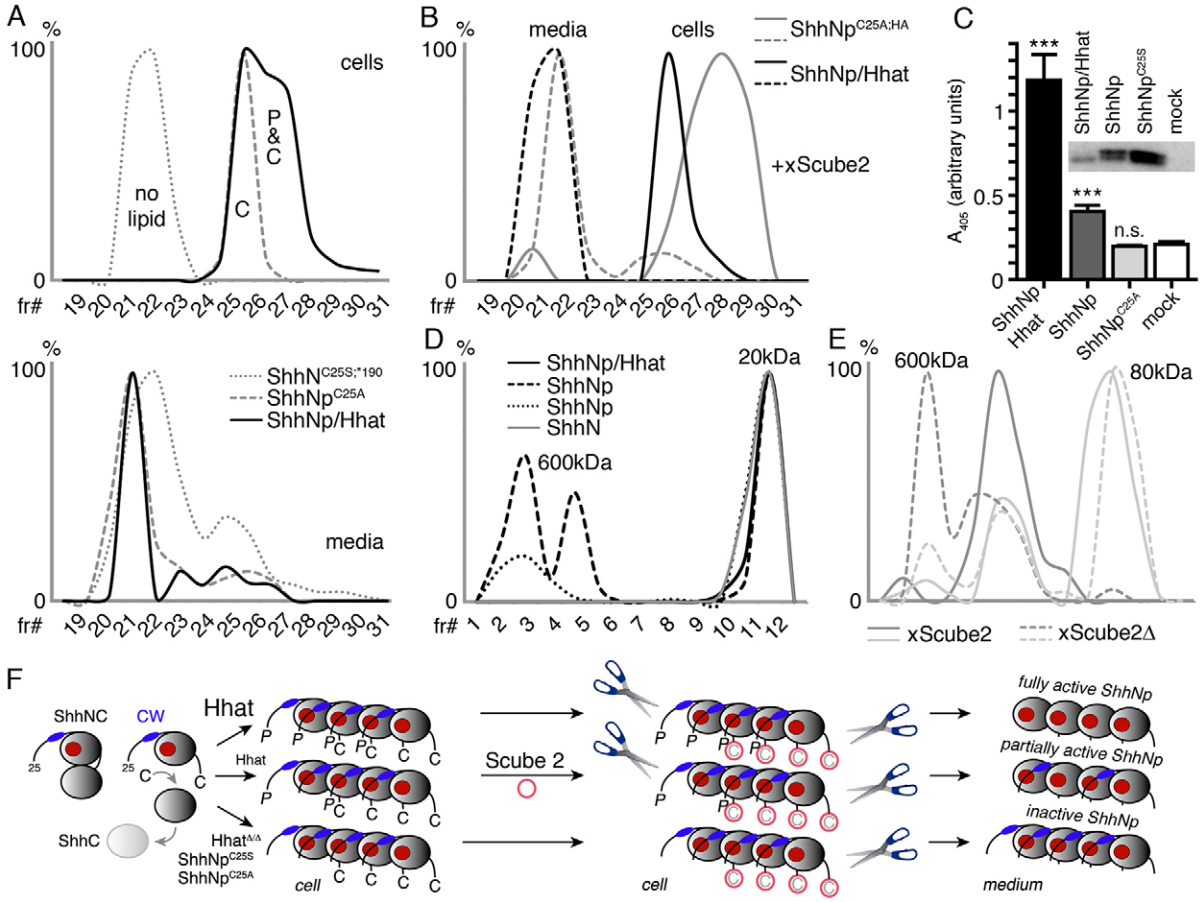

Fig. 8. Solubilized ShhNp lacks both terminal lipids. (A) Reverse-phase HPLC elution profiles of dual-lipidated ShhNp (indicated by 'P&C'), cholesterol-modified ShhNp^{C25A} (indicated by 'C') and truncated unlipidated ShhN$^{C25S;*190}$. In contrast to the cellular forms, the majority of soluble ShhNp/Hhat and ShhNp^{C25A} co-eluted with ShhN$^{C25S;*190}$, demonstrating the loss of both terminal lipids during release (lower panel). Elution profiles are expressed relative to the highest protein amount (set to 100%). (B) Analysis as described in A for proteins coexpressed with xScube2. Solid line, cell bound Shh; dashed line, soluble material. (C) Hhat-coexpressed ShhNp (inset) was strongly bioactive. Data show the means±s.d. ***$P<0.001$; n.s., non-significant. (D,E) Gel-filtration chromatography shows substantial amounts of monomeric ShhNp in solution. By contrast, xScube2 and xScube2Δ were largely multimeric in solution (E). (F) Simplified model for the conversion of membrane-bound ShhNp into soluble proteins. We suggest that surface-tethered ShhNp forms multimeric clusters with the Ptc-binding sites (mostly) blocked. Proteolytic processing results in the removal of inhibitory N-terminal peptides and the activation of Ptc-binding sites. Dispatched-assisted Scube2-mediated extraction of the Shh lipid anchors might prime terminal sheddase target sites for subsequent processing.

knockdown of Ski (Hh) acyltransferase activity *in vivo* (Chamoun et al., 2001). Therefore, any functional analysis of ShhNp release and activation requires a careful choice of expressing cells and culture conditions. To this end, we established an IRES-based Hhat/ShhNp coexpression system that eliminates the post-translational palmitoylation bottleneck and that allowed for the production of authentic, fully biologically active morphogens.

We employed our ShhNp/Hhat coexpression system to test two conflicting concepts of Scube2-mediated ShhNp release (Creanga et al., 2012; Tukachinsky et al., 2012); whereas Creanga et al. reported that palmitoylation enhances mScube2-mediated ShhNp release (Creanga et al., 2012), Tukachinsky et al. showed that the secretion of unrelated HaloTag proteins fused to the cholesterol-esterified eight C-terminal amino acids of Shh was enhanced by xScube2 (Tukachinsky et al., 2012), suggesting that cholesterol is the main determinant for xScube2-dependent ShhNp release. Consistent with this, we observed xScube2-enhanced release of cholesterylated ShhNp^{C25A}, ^{HA}ShhNp^{C25A}, ShhNp$^{C25A;\Delta HA}$ and ShhNp$^{C25A;HA}$ into serum-free medium, but we failed to observe xScube2-dependent solubilization of N-acylated ShhNp/Hhat under various experimental conditions. By contrast, ShhNp/Hhat solubilization was enhanced by mammalian Scube2 (Creanga et al., 2012). Importantly, we observed that both Scube activities were CUB-domain-dependent and were strictly linked to proteolytic substrate processing during release. Thus, we suggest that the Scube2 CUB domain (Tsai et al., 2009; Tukachinsky et al., 2012) might prime cell-tethered morphogens for processing, as has been described for the procollagen C-proteinase enhancers PCPE-1 and PCPE-2 (Blanc et al., 2007). PCPEs are CUB-domain-containing extracellular glycoproteins that stimulate the C-terminal processing of fibrillar procollagens (Blanc et al., 2007; Takahara et al., 1994), but which are devoid of intrinsic proteolytic activity. PCPEs enhance the proteinase activity of tolloid (TLD) by the binding of the CUB-domain to the substrate (Blanc et al., 2007; Takahara et al., 1994). Importantly, this property alone accounts for the enhancing activity of PCPEs. The CUB domain derives its name from complement serine proteinases (C1r, C1s, MASP-1, MASP-2, MASP-3), and bone morphogenetic protein-1 and tolloid metalloproteinases (BMP-1, mTLD, mTLL-1 and mTLL-2) (Blanc et al., 2007). An essential role of CUB domains in these proteins is to mediate protease–protease-substrate complex

assembly (Gaboriaud et al., 2007). These similarities suggest that the function of Scube CUB domains might resemble that of CUB domains in BMP-1/TLD-mediated activation of the transforming growth factor β (TGF-β)-like proteins BMP2 and BMP4 in vertebrates and decapentaplegic (dpp) in arthropods.

Indeed, biochemical and molecular studies have revealed physical interactions between Scube3 CUB domains and TGF-β1 (Yang et al., 2007), and have identified permissive roles of full-length Scube1 on BMP2 activation, possibly through the recruitment of as-yet-unidentified proteases (Tu et al., 2008). Consistent with the latter, the deletion of the Scube1 C-terminal cysteine motif and the CUB domain by targeted disruption in the mouse results in defects in brain patterning that resemble those in mice lacking the BMP antagonist Noggin (McMahon et al., 1998; Tu et al., 2008). Based on these data, we suggest that Scube2 CUB domains might also function in morphogenetic patterning and regulated protease recruitment and activation.

This is supported by the fact that Scube2 activity is a positive component of the Hh pathway *in vivo* (Creanga et al., 2012; Tsai et al., 2009). It is known that the loss of Scube2 activity in the zebrafish embryo leads to mild defects in Hh signal transduction (Hollway et al., 2006), and that simultaneous knockdown of all three Scube genes in triple-morpholino embryos phenocopies a complete loss of embryonic Hh function (Johnson et al., 2012). Notably, impaired Scube function *in vivo* was bypassed by increased ligand expression; the injection of shh mRNA into scube triple-morpholino embryos rescued you-mutant phenotypes, and a moderate (fourfold) increase in shh mRNA induced wild-type-like ectopic expression of Shh target genes in triple-morpholino embryos (Johnson et al., 2012). These *in vivo* observations are incompatible with published models of Scube-mediated Shh extraction and continued association during transport, because any Scube1–3 extraction and transport blockade would not be bypassed by increased amounts of ligand. By contrast, baseline Shh processing in the absence of external regulators is influenced by the frequency of random protease–substrate encounters, which depends on the concentrations of both proteins. Scube enhancer function thus explains the tissue-restricted, mild phenotypes in you-class zebrafish mutants (Kawakami et al., 2005) and in Scube-deficient mice (Tu et al., 2008; Xavier et al., 2013). Finally, Scube enhancer function is consistent with the lack of Scube orthologs in *Drosophila* (Tukachinsky et al., 2012). Thus, we suggest that the transfer of ShhNp from Disp to Scube2 (Tukachinsky et al., 2012) facilitates the proteolytic processing of lipidated Hh peptides. Scube2-mediated release of HaloTag proteins linked to the cholesterylated eight-amino-acid Shh fragment (Tukachinsky et al., 2012) suggests that the Shh globular domain is not required for this process. However, it is conceivable that the emerging dual role of Scube proteins as regulators of opposing Shh and BMP gradients requires common molecular properties that might be sensed by the Scube cysteine-rich and CUB domains.

MATERIALS AND METHODS

Cloning and expression of recombinant proteins

Shh and Hhat constructs were generated from murine cDNA (NM_009170) and human cDNA (BC_117130) by using PCR. PCR products (Shh nucleotides 1–1314, corresponding to amino acids 1–438 of ShhNp; nucleotides 1–594, corresponding to amino acid 1–198 of non-cholesterylated monomeric ShhN; and Hhat nucleotides 1–1481, corresponding to amino acids 1–493) were ligated into pDrive (Qiagen, Hilden, Germany), sequenced, and re-ligated into pcDNA3.1 (Invitrogen, Carlsbad, CA) for the expression of secreted, lipidated 19-kDa ShhNp in Bosc23 cells, which are derived from HEK293 cells. Tagged and untagged *Drosophila* Hh (NM_001038976) was cloned into pUAST-attP (Invitrogen), and was expressed under serum-free conditions in *Drosophila* Schneider S2 cells. $ShhNp^{C25A}$ (Hardy and Resh, 2012) was generated by site-directed mutagenesis (Stratagene, La Jolla, CA). Where indicated, ShhNp was expressed in a hemagglutinin (HA)-tagged form. Primer sequences can be provided upon request. *Xenopus* xScube2 cloned into pCS2+ was a kind gift from Adrian Salic (Tukachinsky et al., 2012), and human Scube2 was a kind gift from Ruey-Bing Yang (Tsai et al., 2009). Hhat cDNA (NM_018194) was obtained from ImaGenes (Berlin, Germany) and cloned into pIRES (ClonTech, Mountain View, CA) for bicistronic ShhNp/Hhat and ShhN/Hhat coexpression in the same transfected cells. This resulted in N-palmitoylated, C-cholesterylated or N-palmitoylated non-cholesterylated proteins, respectively.

Cell culture and protein analysis

Bosc23 cells were cultured in DMEM (PAA, Cölbe, Germany) with 10% fetal calf serum (FCS) and 100 µg/ml penicillin-streptomycin, and they were transfected by using PolyFect (Qiagen). S2 cells were cultured in Schneider's Drosophila medium (Gibco, Darmstadt, Germany) and were transfected using Effectene (Qiagen). CHO-K1 cells were cultured in DMEM/F12 (PAA), and stable Hhat-expressing clones were generated by using G418 selection, followed by the isolation of individual stable transfectants. Cells were cultured for 36 h, the medium was changed and ShhNp was secreted into serum-free medium for various time periods. Where indicated, methyl-β-cyclodextrin (MβCD, Sigma-Aldrich) was added at 100–1000 µg/ml in serum-free DMEM. Proteins that were secreted into serum-free medium were precipitated by using trichloroacetic acid (TCA). All proteins were analyzed by 15% SDS-PAGE, followed by western blotting onto polyvinylidene fluoride (PVDF) membranes. Ponceau S staining of PVDF membranes after blotting or Coomassie staining of gels were performed as loading controls. Blotted proteins were detected by using monoclonal α-HA antibodies (mouse IgG, Sigma, St Louis, MO), polyclonal α-FLAG antibodies (Sigma), polyclonal α-Shh antibodies (goat IgG; R&D Systems, Minneapolis, MN) or polyclonal α-CW antibodies directed against the heparan sulfate (HS)-binding CW sequence (rabbit IgG, Cell Signaling, Beverly, MA). Incubation with peroxidase-conjugated donkey-α-goat-, donkey-α-rabbit- or donkey-α-mouse-IgG (Dianova, Hamburg, Germany) was followed by chemiluminescent detection (Pierce). Photoshop was used to convert grayscale blots into merged RGB pictures for improved visualization and quantification of N- and C-terminal peptide processing (α-Shh-detected proteins were always labeled green, α-CW-detected proteins were red and HA-tags were blue).

Chromatography

Unimpaired $ShhNp^{C25A}$ multimerization upon expression in Bosc23 cells was confirmed by gel-filtration analysis using a Superdex200 10/300 GL column (GE Healthcare, Chalfont St Giles, UK) equilibrated with PBS at 4°C for fast protein liquid chromatography (FPLC) [Äkta Protein Purifier (GE Healthcare)]. Eluted fractions were TCA precipitated, resolved by 15% SDS-PAGE and immunoblotted. Signals were quantified by using ImageJ. Reverse-phase HPLC was performed as described previously (Pepinsky et al., 1998), on a C4-300 column (Tosoh, Tokyo, Japan) and an Äkta Basic P900 Protein Purifier. Briefly, Bosc23 cells were transfected with expression plasmids for Shh and monolipidated or unlipidated mutants. At 2 days post transfection, cells were lyzed on ice in RIPA buffer containing complete protease inhibitor cocktail (Roche, Basel, Switzerland), ultracentrifuged, and the soluble whole-cell extract was acetone precipitated. Serum-free media obtained after overnight Shh expression were treated in the same way. Protein precipitates were resuspended in 35 µl of 1,1,1,3,3,3-hexafluoro-2-propanol and solubilized with 70 µl of 70% formic acid, followed by sonication. For reverse-phase HPLC, a 0–70% acetonitrile-water gradient containing 0.1% trifluoroacetic acid was used at room temperature for 30 min. Elution samples were vacuum dried, resolubilized in reducing sample

buffer, and analyzed by SDS-PAGE and immunoblotting. Signals were quantified using ImageJ.

Shh reporter assays

C3H10T1/2 cells (Nakamura et al., 1997) were grown in DMEM supplemented with 10% FCS and antibiotics. At 24 h after seeding, Shh-conditioned media were mixed 1:1 with DMEM containing 10% FCS and antibiotics, and were applied to C3H10T1/2 cells in 15-mm plates. To some samples, 2.5 µM cyclopamine, a specific inhibitor of Shh signaling, and 1 µg/ml of Shh-neutralizing antibody 5E1 (Ericson et al., 1996) were added as controls to confirm the specificity of the assay. Generally, owing to variable expression levels, mutant and wild-type proteins were adjusted to comparable levels before the induction of C3H10T1/2 differentiation. Cells were lysed at 5–6 days after induction (in 20 mM HEPES, 150 mM NaCl, 0.5% Triton X-100, pH 7.4), and osteoblast-specific alkaline phosphatase activity was measured at 405 nm after the addition of 120 mM para-nitrophenolphosphate (Sigma) in 0.1M glycine buffer, pH 9.5. Assays were always performed in triplicate.

RT-PCR

For RT-PCR analysis of *Disp*, *Scube* and *Hhat* mRNA expression, TriZol reagent (Invitrogen) was used for RNA extraction from various cultured cell types, and a first strand DNA synthesis kit (Thermo, Schwerte, Germany) was used for cDNA synthesis. PCR was performed by running 35 cycles using intron-spanning species-specific primer pairs (sequences can be provided upon request). Scube2 PCR was performed by running 40 cycles. In some cases, nested PCR was conducted to further amplify the signal.

Statistical analysis

Proteins on blots were quantified by using ImageJ. Relative protein release in a given experiment was calculated following quantification as the amount of solubilized protein divided by cellular expression, and was expressed as a percentage (soluble protein/corresponding cellular protein×100). All statistical analysis was performed in Prism using Student's *t*-test (two-tailed, unpaired, CI 95%). All error estimates are standard deviations of the mean (s.d.).

Bioinformatics

The crystal structure of murine Shh (Protein Data Bank ID 1VHH) (Hall et al., 1995) was displayed by using the PyMOL Molecular Graphics System, v1.3, Schrödinger, LLC. Physicochemical parameters of HA amino acids and Shh C-terminal amino acids were determined using ProtParam. CLC Sequence Viewer 5 was used for sequence visualization.

Acknowledgements

xScube2 expression constructs were kindly provided by Hanna Tukachinsky and Adrian Salic (Harvard Medical School, Boston, MA), hScube2 constructs by Ming-Tzu Tsai and Ruey-Bing Yang (Academia Sinica, Taipei, Taiwan), and Hhat constructs by Marilyn Resh (Sloan-Kettering Center, New York, NY). The authors thank Lydia Sorokin (Westfälische Wilhelms Universität Münster, Münster, Germany) for critical proofreading.

Competing interests

The authors declare no competing interests.

Author contributions

P.J., S.E., S.S., U.P., C.O., S.B., S.K., P.S., U.H. and K.G. performed experiments; U.P., D.G.S. and K.G. conceived experiments; and K.G. wrote the paper.

Funding

This work was supported by Deutsche Forschungsgemeinschaft (DFG) fellowships [grant numbers GRK1549/1 to U.P., S.B., C.O. and P.J.; and GR1748/4-1 to K.G.]; and the Innovative Medical Research fund of the University of Münster Medical School [DR111108].

Supplementary material

Supplementary material available online at
http://jcs.biologists.org/lookup/suppl/doi:10.1242/jcs.137695/-/DC1

References

Ahn, S. and Joyner, A. L. (2004). Dynamic changes in the response of cells to positive hedgehog signaling during mouse limb patterning. *Cell* **118**, 505-516.
Amanai, K. and Jiang, J. (2001). Distinct roles of Central missing and Dispatched in sending the Hedgehog signal. *Development* **128**, 5119-5127.
Bischoff, M., Gradilla, A. C., Seijo, I., Andrés, G., Rodríguez-Navas, C., González-Méndez, L. and Guerrero, I. (2013). Cytonemes are required for the establishment of a normal Hedgehog morphogen gradient in Drosophila epithelia. *Nat. Cell Biol.* **15**, 1269-1281.
Bishop, B., Aricescu, A. R., Harlos, K., O'Callaghan, C. A., Jones, E. Y. and Siebold, C. (2009). Structural insights into hedgehog ligand sequestration by the human hedgehog-interacting protein HHIP. *Nat. Struct. Mol. Biol.* **16**, 698-703.
Blanc, G., Font, B., Eichenberger, D., Moreau, C., Ricard-Blum, S., Hulmes, D. J. and Moali, C. (2007). Insights into how CUB domains can exert specific functions while sharing a common fold: conserved and specific features of the CUB1 domain contribute to the molecular basis of procollagen C-proteinase enhancer-1 activity. *J. Biol. Chem.* **282**, 16924-16933.
Bosanac, I., Maun, H. R., Scales, S. J., Wen, X., Lingel, A., Bazan, J. F., de Sauvage, F. J., Hymowitz, S. G. and Lazarus, R. A. (2009). The structure of SHH in complex with HHIP reveals a recognition role for the Shh pseudo active site in signaling. *Nat. Struct. Mol. Biol.* **16**, 691-697.
Briscoe, J., Chen, Y., Jessell, T. M. and Struhl, G. (2001). A hedgehog-insensitive form of patched provides evidence for direct long-range morphogen activity of sonic hedgehog in the neural tube. *Mol. Cell* **7**, 1279-1291.
Bumcrot, D. A., Takada, R. and McMahon, A. P. (1995). Proteolytic processing yields two secreted forms of sonic hedgehog. *Mol. Cell. Biol.* **15**, 2294-2303.
Chamoun, Z., Mann, R. K., Nellen, D., von Kessler, D. P., Bellotto, M., Beachy, P. A. and Basler, K. (2001). Skinny hedgehog, an acyltransferase required for palmitoylation and activity of the hedgehog signal. *Science* **293**, 2080-2084.
Chang, S. C., Mulloy, B., Magee, A. I. and Couchman, J. R. (2011). Two distinct sites in sonic Hedgehog combine for heparan sulfate interactions and cell signaling functions. *J. Biol. Chem.* **286**, 44391-44402.
Charron, F., Stein, E., Jeong, J., McMahon, A. P. and Tessier-Lavigne, M. (2003). The morphogen sonic hedgehog is an axonal chemoattractant that collaborates with netrin-1 in midline axon guidance. *Cell* **113**, 11-23.
Chen, M. H., Li, Y. J., Kawakami, T., Xu, S. M. and Chuang, P. T. (2004). Palmitoylation is required for the production of a soluble multimeric Hedgehog protein complex and long-range signaling in vertebrates. *Genes Dev.* **18**, 641-659.
Creanga, A., Glenn, T. D., Mann, R. K., Saunders, A. M., Talbot, W. S. and Beachy, P. A. (2012). Scube/You activity mediates release of dually lipid-modified Hedgehog signal in soluble form. *Genes Dev.* **26**, 1312-1325.
Dierker, T., Dreier, R., Petersen, A., Bordych, C. and Grobe, K. (2009). Heparan sulfate-modulated, metalloprotease-mediated sonic hedgehog release from producing cells. *J. Biol. Chem.* **284**, 8013-8022.
Ericson, J., Morton, S., Kawakami, A., Roelink, H. and Jessell, T. M. (1996). Two critical periods of Sonic Hedgehog signaling required for the specification of motor neuron identity. *Cell* **87**, 661-673.
Farshi, P., Ohlig, S., Pickhinke, U., Höing, S., Jochmann, K., Lawrence, R., Dreier, R., Dierker, T. and Grobe, K. (2011). Dual roles of the Cardin-Weintraub motif in multimeric Sonic hedgehog. *J. Biol. Chem.* **286**, 23608-23619.
Gaboriaud, C., Teillet, F., Gregory, L. A., Thielens, N. M. and Arlaud, G. J. (2007). Assembly of C1 and the MBL- and ficolin-MASP complexes: structural insights. *Immunobiology* **212**, 279-288.
Guerrero, I. and Chiang, C. (2007). A conserved mechanism of Hedgehog gradient formation by lipid modifications. *Trends Cell Biol.* **17**, 1-5.
Hall, T. M., Porter, J. A., Beachy, P. A. and Leahy, D. J. (1995). A potential catalytic site revealed by the 1.7-A crystal structure of the amino-terminal signalling domain of Sonic hedgehog. *Nature* **378**, 212-216.
Hardy, R. Y. and Resh, M. D. (2012). Identification of N-terminal residues of Sonic Hedgehog important for palmitoylation by Hedgehog acyltransferase. *J. Biol. Chem.* **287**, 42881-42889.
Harfe, B. D., Scherz, P. J., Nissim, S., Tian, H., McMahon, A. P. and Tabin, C. J. (2004). Evidence for an expansion-based temporal Shh gradient in specifying vertebrate digit identities. *Cell* **118**, 517-528.
Hollway, G. E., Maule, J., Gautier, P., Evans, T. M., Keenan, D. G., Lohs, C., Fischer, D., Wicking, C. and Currie, P. D. (2006). Scube2 mediates Hedgehog signalling in the zebrafish embryo. *Dev. Biol.* **294**, 104-118.
Johnson, J. L., Hall, T. E., Dyson, J. M., Sonntag, C., Ayers, K., Berger, S., Gautier, P., Mitchell, C., Hollway, G. E. and Currie, P. D. (2012). Scube activity is necessary for Hedgehog signal transduction in vivo. *Dev. Biol.* **368**, 193-202.
Kawakami, A., Nojima, Y., Toyoda, A., Takahoko, M., Satoh, M., Tanaka, H., Wada, H., Masai, I., Terasaki, H., Sakaki, Y. et al. (2005). The zebrafish-secreted matrix protein you/scube2 is implicated in long-range regulation of hedgehog signaling. *Curr. Biol.* **15**, 480-488.
Kojro, E., Gimpl, G., Lammich, S., Marz, W. and Fahrenholz, F. (2001). Low cholesterol stimulates the nonamyloidogenic pathway by its effect on the alpha -secretase ADAM 10. *Proc. Natl. Acad. Sci. USA* **98**, 5815-5820.
Lee, J. D. and Treisman, J. E. (2001). Sightless has homology to transmembrane acyltransferases and is required to generate active Hedgehog protein. *Curr. Biol.* **11**, 1147-1152.
Lee, J. J., Ekker, S. C., von Kessler, D. P., Porter, J. A., Sun, B. I. and Beachy, P. A. (1994). Autoproteolysis in hedgehog protein biogenesis. *Science* **266**, 1528-1537.

Lee, J. D., Kraus, P., Gaiano, N., Nery, S., Kohtz, J., Fishell, G., Loomis, C. A. and Treisman, J. E. (2001). An acylatable residue of Hedgehog is differentially required in Drosophila and mouse limb development. *Dev. Biol.* **233**, 122-136.
Liu, X. Q. (2000). Protein-splicing intein: Genetic mobility, origin, and evolution. *Annu. Rev. Genet.* **34**, 61-76.
Martí, E., Bumcrot, D. A., Takada, R. and McMahon, A. P. (1995). Requirement of 19K form of Sonic hedgehog for induction of distinct ventral cell types in CNS explants. *Nature* **375**, 322-325.
Matthews, V., Schuster, B., Schütze, S., Bussmeyer, I., Ludwig, A., Hundhausen, C., Sadowski, T., Saftig, P., Hartmann, D., Kallen, K. J. et al. (2003). Cellular cholesterol depletion triggers shedding of the human interleukin-6 receptor by ADAM10 and ADAM17 (TACE). *J. Biol. Chem.* **278**, 38829-38839.
McMahon, J. A., Takada, S., Zimmerman, L. B., Fan, C. M., Harland, R. M. and McMahon, A. P. (1998). Noggin-mediated antagonism of BMP signaling is required for growth and patterning of the neural tube and somite. *Genes Dev.* **12**, 1438-1452.
Micchelli, C. A., The, I., Selva, E., Mogila, V. and Perrimon, N. (2002). Rasp, a putative transmembrane acyltransferase, is required for Hedgehog signaling. *Development* **129**, 843-851.
Miura, G. I., Buglino, J., Alvarado, D., Lemmon, M. A., Resh, M. D. and Treisman, J. E. (2006). Palmitoylation of the EGFR ligand Spitz by Rasp increases Spitz activity by restricting its diffusion. *Dev. Cell* **10**, 167-176.
Nakamura, T., Aikawa, T., Iwamoto-Enomoto, M., Iwamoto, M., Higuchi, Y., Pacifici, M., Kinto, N., Yamaguchi, A., Noji, S., Kurisu, K. et al. (1997). Induction of osteogenic differentiation by hedgehog proteins. *Biochem. Biophys. Res. Commun.* **237**, 465-469.
Nishie, W., Jackow, J., Hofmann, S. C., Franzke, C. W. and Bruckner-Tuderman, L. (2012). Coiled coils ensure the physiological ectodomain shedding of collagen XVII. *J. Biol. Chem.* **287**, 29940-29948.
Ohlig, S., Farshi, P., Pickhinke, U., van den Boom, J., Höing, S., Jakuschev, S., Hoffmann, D., Dreier, R., Schöler, H. R., Dierker, T. et al. (2011). Sonic hedgehog shedding results in functional activation of the solubilized protein. *Dev. Cell* **20**, 764-774.
Ohlig, S., Pickhinke, U., Sirko, S., Bandari, S., Hoffmann, D., Dreier, R., Farshi, P., Götz, M. and Grobe, K. (2012). An emerging role of Sonic hedgehog shedding as a modulator of heparan sulfate interactions. *J. Biol. Chem.* **287**, 43708-43719.
Palm, W., Swierczynska, M. M., Kumari, V., Ehrhart-Bornstein, M., Bornstein, S. R. and Eaton, S. (2013). Secretion and signaling activities of lipoprotein-associated hedgehog and non-sterol-modified hedgehog in flies and mammals. *PLoS Biol.* **11**, e1001505.
Panáková, D., Sprong, H., Marois, E., Thiele, C. and Eaton, S. (2005). Lipoprotein particles are required for Hedgehog and Wingless signalling. *Nature* **435**, 58-65.
Parkin, E. T., Watt, N. T., Turner, A. J. and Hooper, N. M. (2004). Dual mechanisms for shedding of the cellular prion protein. *J. Biol. Chem.* **279**, 11170-11178.
Pepinsky, R. B., Zeng, C., Wen, D., Rayhorn, P., Baker, D. P., Williams, K. P., Bixler, S. A., Ambrose, C. M., Garber, E. A., Miatkowski, K. et al. (1998). Identification of a palmitic acid-modified form of human Sonic hedgehog. *J. Biol. Chem.* **273**, 14037-14045.
Peters, C., Wolf, A., Wagner, M., Kuhlmann, J. and Waldmann, H. (2004). The cholesterol membrane anchor of the Hedgehog protein confers stable membrane association to lipid-modified proteins. *Proc. Natl. Acad. Sci. USA* **101**, 8531-8536.
Porter, J. A., Ekker, S. C., Park, W. J., von Kessler, D. P., Young, K. E., Chen, C. H., Ma, Y., Woods, A. S., Cotter, R. J., Koonin, E. V. et al. (1996a). Hedgehog patterning activity: role of a lipophilic modification mediated by the carboxy-terminal autoprocessing domain. *Cell* **86**, 21-34.
Porter, J. A., Young, K. E. and Beachy, P. A. (1996b). Cholesterol modification of hedgehog signaling proteins in animal development. *Science* **274**, 255-259.
Roy, S., Hsiung, F. and Kornberg, T. B. (2011). Specificity of Drosophila cytonemes for distinct signaling pathways. *Science* **332**, 354-358.
Schauerte, H. E., van Eeden, F. J., Fricke, C., Odenthal, J., Strähle, U. and Haffter, P. (1998). Sonic hedgehog is not required for the induction of medial floor plate cells in the zebrafish. *Development* **125**, 2983-2993.
Tabata, T. and Kornberg, T. B. (1994). Hedgehog is a signaling protein with a key role in patterning Drosophila imaginal discs. *Cell* **76**, 89-102.
Taipale, J., Chen, J. K., Cooper, M. K., Wang, B., Mann, R. K., Milenkovic, L., Scott, M. P. and Beachy, P. A. (2000). Effects of oncogenic mutations in Smoothened and Patched can be reversed by cyclopamine. *Nature* **406**, 1005-1009.
Takahara, K., Kessler, E., Biniaminov, L., Brusel, M., Eddy, R. L., Jani-Sait, S., Shows, T. B. and Greenspan, D. S. (1994). Type I procollagen COOH-terminal proteinase enhancer protein: identification, primary structure, and chromosomal localization of the cognate human gene (PCOLCE). *J. Biol. Chem.* **269**, 26280-26285.
Theunissen, J. W. and de Sauvage, F. J. (2009). Paracrine Hedgehog signaling in cancer. *Cancer Res.* **69**, 6007-6010.
Tsai, M. T., Cheng, C. J., Lin, Y. C., Chen, C. C., Wu, A. R., Wu, M. T., Hsu, C. C. and Yang, R. B. (2009). Isolation and characterization of a secreted, cell-surface glycoprotein SCUBE2 from humans. *Biochem. J.* **422**, 119-128.
Tu, C. F., Yan, Y. T., Wu, S. Y., Djoko, B., Tsai, M. T., Cheng, C. J. and Yang, R. B. (2008). Domain and functional analysis of a novel platelet-endothelial cell surface protein, SCUBE1. *J. Biol. Chem.* **283**, 12478-12488.
Tukachinsky, H., Kuzmickas, R. P., Jao, C. Y., Liu, J. and Salic, A. (2012). Dispatched and scube mediate the efficient secretion of the cholesterol-modified hedgehog ligand. *Cell Rep.* **2**, 308-320.
von Tresckow, B., Kallen, K. J., von Strandmann, E. P., Borchmann, P., Lange, H., Engert, A. and Hansen, H. P. (2004). Depletion of cellular cholesterol and lipid rafts increases shedding of CD30. *J. Immunol.* **172**, 4324-4331.
Vyas, N., Goswami, D., Manonmani, A., Sharma, P., Ranganath, H. A., VijayRaghavan, K., Shashidhara, L. S., Sowdhamini, R. and Mayor, S. (2008). Nanoscale organization of hedgehog is essential for long-range signaling. *Cell* **133**, 1214-1227.
Walev, I., Tappe, D., Gulbins, E. and Bhakdi, S. (2000). Streptolysin O-permeabilized granulocytes shed L-selectin concomitantly with ceramide generation via neutral sphingomyelinase. *J. Leukoc. Biol.* **68**, 865-872.
Xavier, G. M., Panousopoulos, L. and Cobourne, M. T. (2013). Scube3 is expressed in multiple tissues during development but is dispensable for embryonic survival in the mouse. *PLoS ONE* **8**, e55274.
Yang, H. Y., Cheng, C. F., Djoko, B., Lian, W. S., Tu, C. F., Tsai, M. T., Chen, Y. H., Chen, C. C., Cheng, C. J. and Yang, R. B. (2007). Transgenic overexpression of the secreted, extracellular EGF-CUB domain-containing protein SCUBE3 induces cardiac hypertrophy in mice. *Cardiovasc. Res.* **75**, 139-147.
Yauch, R. L., Gould, S. E., Scales, S. J., Tang, T., Tian, H., Ahn, C. P., Marshall, D., Fu, L., Januario, T., Kallop, D. et al. (2008). A paracrine requirement for hedgehog signalling in cancer. *Nature* **455**, 406-410.
Zhao, C., Chen, A., Jamieson, C. H., Fereshteh, M., Abrahamsson, A., Blum, J., Kwon, H. Y., Kim, J., Chute, J. P., Rizzieri, D. et al. (2009). Hedgehog signalling is essential for maintenance of cancer stem cells in myeloid leukaemia. *Nature* **458**, 776-779.
Zimina, E. P., Bruckner-Tuderman, L. and Franzke, C. W. (2005). Shedding of collagen XVII ectodomain depends on plasma membrane microenvironment. *J. Biol. Chem.* **280**, 34019-34024.